Segregation and trapping of erbium at a moving crystal-amorphous Si interface

A. Polman, J. S. Custer, P. M. Zagwijn, and A. M. Molenbroek
FOM-Institute for Atomic and Molecular Physics, Kruislaan 407, 1098 SJ Amsterdam, The Netherlands

P. F. A. Alkemade
DIMES/NF, Faculty of Applied Physics, Delft University of Technology, Lorentzweg 1, 2628 CJ Delft, The Netherlands

(Received 29 April 1996; accepted for publication 27 September 1996)

Segregation and trapping of Er during solid-phase crystallization of amorphous Si on crystalline Si is studied in a concentration range of 10^{16}–5×10^{20} Er/cm^3. Amorphous surface layers are prepared on Si(100) by 250 keV Er ion implantation, recrystallized at 600 °C, and then analyzed using high-resolution Rutherford backscattering spectrometry using 2 MeV He^+ or 100 keV H^+. The segregation coefficient k depends strongly on Er concentration. At Er interface areal densities below 6×10^{13} Er/cm^2 nearly full segregation to the surface is observed, with $k=0.01$. At higher Er densities, segregation and trapping in the crystal are observed, with $k=0.20$. The results are consistent with a model in which it is assumed that defects in the a-Si near the interface act as traps for the Er. © *1997 American Institute of Physics.* [S0021-8979(97)04601-X]

I. INTRODUCTION

Solid phase epitaxial crystallization (SPE) of amorphous (a-Si) on a crystalline Si (c-Si) substrate proceeds in a layer-by-layer fashion, with bond rearrangements presumably taking place at ledges at the growing crystal face, at a singly activated (2.68 eV) rate and a typical growth velocity at 600 °C of 1 nm/s.[1] In the presence of impurities, crystallization often results in segregation, the redistribution of the impurity at the moving phase boundary. In general, the segregation is characterized by a segregation coefficient k, defined as the ratio of the impurity concentrations on either side of the interface. Previous examples of impurity segregation in Si during SPE can be split in two different cases: (1) impurities with very low diffusivity (B, P, As, Sb), which show no or only very small redistribution, resulting in complete trapping in the growing crystal, often at concentrations well above the equilibrium solubility,[2,3] (2) fast diffusers (Cu, Ag, Au), with very low solubility in c-Si, which can readily escape from the growing crystal, with (nearly) no trapping.[4,5] All experiments on these two classes of impurities have been described in terms of a kinetic segregation and trapping process, determined by the bulk diffusivities of the impurities in a-Si and a nonequilibrium segregation coefficient.

Recently, we have studied the segregation and trapping of erbium in Si, which show a behavior completely different than what has so far been observed for all other impurities.[6,7] Er-doped silicon is an interesting optoelectronic material, due to optical transitions in the internal $4f$ shell of Er^{3+},[8] and in order to fully exploit the possibilities of this material, detailed knowledge of the incorporation behavior of Er in Si is required. The equilibrium solubility of Er in c-Si is unknown, but by analogy to the transition metals[9] it is estimated to be 10^{14}–10^{16} cm^{-3}. We have previously shown that during SPE, Er shows both segregation and trapping (up to concentrations of 2×10^{20} Er/cm^3), an intermediate behavior with respect to the two cases mentioned above. However, the detailed mechanism by which this unusual segregation process proceeds has remained unclear. We have suggested a model[7] in which it is assumed that defects in the amorphous Si near the interface can act as traps for the Er and thereby affect the partitioning of Er at the a-Si/c-Si interface. To test this model, we present in this paper measurements of the Er concentration dependence of segregation and trapping of Er in Si, in a concentration range of more than 4 orders of magnitude (10^{16}–5×10^{20} Er/cm^3), including high resolution measurements of the Er segregation profile around the a-Si/c-Si interface. The segregation coefficient depends strongly on Er concentration. The results are consistent with the defect trapping model.

II. EXPERIMENT

Erbium was implanted into single-crystal Czochralski-grown Si(100) at 90 K. Fluences of 6×10^{13}, 3×10^{14}, and 9×10^{14} Er^+/cm^2 were used, at an energy of 250 keV. These doses resulted in full amorphization of a surface layer of ≈140 nm thickness, with Er profiles confined in the amorphous layer. A second set of 250 keV implants, at fluences of 7×10^{12}, 7×10^{13}, and 7×10^{14} Er/cm^2 was performed in Czochralski-grown Si(100) wafers which were preamorphized by a 350 keV Si^+ implant at 90 K (amorphous layer thickness 350 nm). The Er-doped a-Si layers were recrystallized at 600 °C in a standard vacuum tube furnace at a base pressure of 10^{-6} mbar. Some samples were recrystallized using a rapid thermal annealing (RTA) furnace at 600 °C in N_2 at 1 bar.

Before and after annealing, samples were analyzed using Rutherford backscattering spectrometry (RBS) using 2 MeV He^+ at a scattering angle of 100°, using a surface barrier detector with an energy resolution of 14 keV. Some samples were analyzed with better depth resolution using 100 keV H^+ RBS around a scattering angle of 105°. A toroidal electrostatic analyzer[10] was used with an energy resolution $\Delta E/E=9\times10^{-4}$. All RBS energy spectra were converted to depth scales using known stopping powers. The depth reso-

Downloaded¬15¬Sep¬2003¬to¬131.215.237.132.¬Redistribution¬subject¬to¬AIP¬license¬or¬copyright,¬see¬http://ojps.aip.org/japo/japcr.jsp

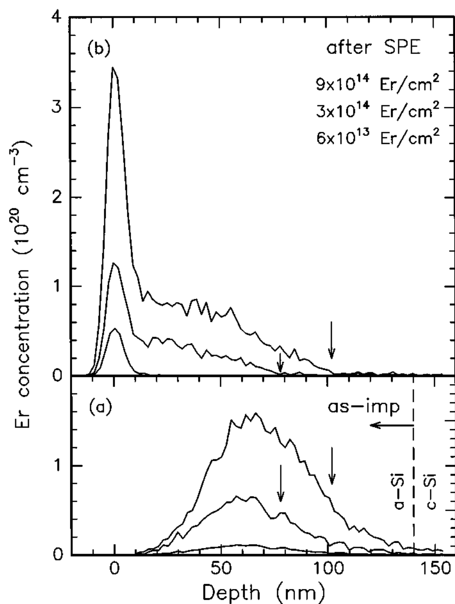

FIG. 1. Erbium concentration depth profiles derived from 2 MeV He^+ RBS data. Results are shown for 6×10^{13}, 3×10^{14}, and 9×10^{14} 250 keV Er/cm^2, implanted in Si(100); (a) as-implanted, (b) after SPE at 600 °C for 15 min.

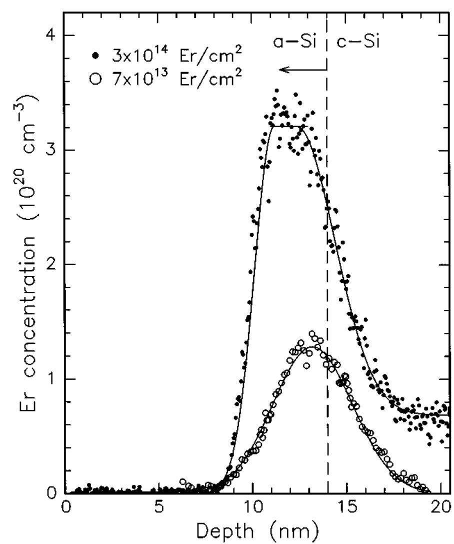

FIG. 2. Erbium concentration depth profiles derived from 100 keV H^+ RBS data. Results are shown for amorphous layers implanted with 7×10^{13} and 3×10^{14} 250 keV Er/cm^2, and annealed in a RTA furnace at 600 °C for 40 s. This anneal causes epitaxial recrystallization of nearly the whole film, with a 14 nm thick amorphous layer remaining at the surface. The solid lines serve to guide the eye.

lutions were 10 nm for the high energy RBS and ranging from 0.2 to 2 nm (depending on the depth) for the low energy RBS measurements. Concentration scales were determined using known scattering cross section for Er. Secondary ion mass spectrometry (SIMS) was performed on some samples to detect low levels of Er. A 6 keV O_2^+ sputter beam was used in ultrahigh vacuum. Secondary ion intensities were converted to atomic densities using known relative sensitivity factors.[11]

III. RESULTS

Figure 1(a) shows the as-implanted Er depth profiles after 6×10^{13}, 3×10^{14}, and 9×10^{14} Er/cm^2 implantation at 250 keV. The implantation profiles are Gaussian in shape with a full width at half-maximum of 60 nm and a peak concentration ranging from 1.0×10^{19} to 1.5×10^{20} Er/cm^3. The depth of the amorphous-crystal interface (determined from the Si part of channeling spectra) is indicated by the dashed line. Erbium depth profiles after annealing for 15 min at 600 °C are shown in Fig. 1(b). Channeling data (not shown) indicate that in all three cases the amorphous layer has fully recrystallized and perfect epitaxy is achieved. No difference was observed between Er depth profiles taken in random or channeling geometry, indicating the Er is not on substitutional nor on tetrahedral interstitial sites.

The data in Fig. 1 clearly show that after SPE, Er is segregated towards the surface, with some fraction of the Er being trapped in the crystal. The trapping behavior depends strongly on Er concentration: for the lowest fluence no trapping is observed (as far as can be detected by RBS: detection limit$=2\times10^{18}$ Er/cm^3) and all Er is segregated to the surface. For the intermediate fluence no trapping is observed in the region between the original *a*-Si/*c*-Si interface and a depth of roughly 80 nm. A gradual increase in the Er concentration is observed from 80 nm depth towards the surface, with a trapped Er concentration just below the surface of 4×10^{19} Er/cm^3. For the highest fluence, the trapping starts at a depth of 100 nm, and the trapped Er concentration increases up to 1×10^{20} Er/cm^3 just below the surface. Note that for the two highest fluence samples, as the interface moves towards the surface, the transition from no trapping to trapping [indicated by arrows in Fig. 1(b)] is quite abrupt, and occurs at a depth at which a significant part of the Er in the original amorphous layer [see Fig. 1(a), where corresponding arrows are also shown] has been rejected from the growing crystal.

To study the segregation process and its concentration dependence in more detail, high resolution RBS measurements were performed on partially recrystallized samples. RTA anneals were performed at 600 °C for 40 s, a time which was chosen such that only 14 nm of the original amorphous layer remained. This surface layer is so thin that the Er segregation profile around the interface can be accurately measured using RBS with 100 keV H^+. Erbium depth profiles were measured for two implantation fluences: 7×10^{13} [no trapping, see Fig. 1(b)] and 3×10^{14} Er/cm^2 [trapping from 80 nm depth to the surface, see Fig. 1(b)] and are shown in Fig. 2. The position of the amorphous-crystal interface was determined from the edge in the Si part of channeling spectra, and is indicated as a dashed line in Fig. 2. The width of this edge was also determined and corresponds to standard deviations of $\sigma=1.1$ nm and $\sigma=1.9$ nm for the high- and low-dose sample, respectively. These values, which are due to straggle and interface roughness, determine the depth resolution of the Er profiles around the interface in Fig. 2. The fact that they are different must be due to a difference in interface roughness, which is either intrinsic to the different Er concentrations or due to temperature inhomogeneities across the sample during annealing resulting in an inhomogeneous *a*-Si layer thickness after SPE.

Downloaded¬15¬Sep¬2003¬to¬131.215.237.132.¬Redistribution¬subject¬to¬AIP¬license¬or¬copyright,¬see¬http://ojps.aip.org/japo/japcr.jsp

Both spectra show an Er segregation spike at the amorphous side of the interface. For the lowest fluence sample no trapping is observed in the crystal, consistent with Fig. 1(b). Only a tail is observed in the crystal near the interface. For the higher fluence, significant trapping in the crystal is observed, also consistent with Fig. 1(b). Correcting the profile for the low-fluence sample (with a width $\sigma=2.1$ nm) for the depth resolution at that depth ($\sigma=1.9$ nm), we find a deconvoluted spike width of $\sigma=0.9$ nm, and a peak concentration of 3×10^{20} cm^{-3}.

The profile for the high-fluence sample shows much more structure than that for the low-fluence sample. A ≈3 nm thick region of roughly constant Er concentration is observed at the amorphous side of the interface. All segregated Er is confined in this narrow region, with no long range diffusion towards the surface. The edge around a depth of 10 nm has a width identical to the depth resolution ($\sigma=1.1$ nm), and is therefore very sharp. These data indicate that Er is diffusing relatively fast in a thin region at the amorphous side of the interface where the Er concentration is high.

From the data in Fig. 1 it is possible to determine a relation between the Er density in the segregation spike at a certain depth and the Er concentration that is trapped at that depth. To do this, the data for the three fluences in Fig. 1 were each analyzed in the following way. The as-implanted Er profile in Fig. 1(a) was first integrated from the initial amorphous-crystal interface depth (140 nm) to a certain depth $d(<140$ nm). The same was done for the corresponding Er profile after SPE in Fig. 1(b). The two integrated values were then subtracted to yield the Er areal density in the segregation spike at the interface after regrowth to a depth d. This procedure was performed for all depths $d=20$–150 nm. As the Er concentration trapped in the crystal is also known for $d=20$–150 nm [Fig. 1(b)], a data set could then be derived for the trapped Er concentration as a function of Er interfacial density. This procedure was followed for the three fluences in Fig. 1 and the three data sets are shown in Fig. 3.

The data for the highest fluence implants (9×10^{14} Er/cm^2, open circles in Fig. 3) show no trapping for low interface concentration, but above a threshold of $\approx6\times10^{13}$ Er/cm^2 at the interface, the trapped Er concentration abruptly increases. The increase is roughly linear with interface concentration. Data for the 3×10^{14} sample are also overlaid (crosses) and show the same behavior, with the same threshold at 6×10^{13} Er/cm^2. Finally, data for the lowest fluence sample, 6×10^{13} Er/cm^2, are also included (closed circles) and all lie in the left-bottom corner of the figure. Indeed, this implanted Er fluence is equal to the threshold fluence and no trapping was observed.

To study the low-concentration behavior in more detail, SIMS measurements were performed on amorphous surface layers implanted with 7×10^{12}, 7×10^{13}, or 7×10^{14}, Er/cm^2, recrystallized at 600 °C. Er depth profiles after SPE are shown in Fig. 4. As SIMS is a much more concentration-sensitive technique than RBS, low concentrations of Er trapped in the crystal, which were not detected in Figs. 1 and 2 for the low-dose samples, are now observed. The depth profiles for the two lowest fluence samples are identical,

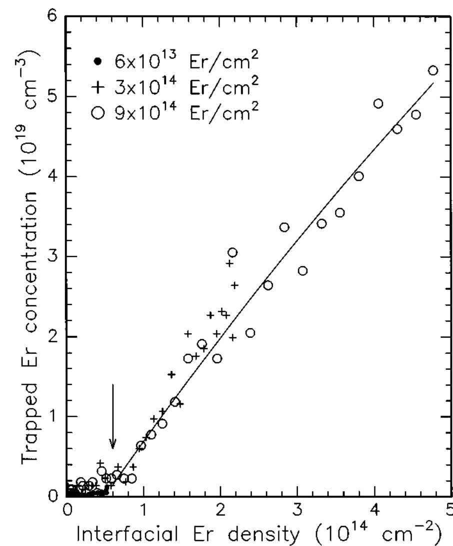

FIG. 3. Trapped Er concentration as a function of Er areal density at the a-Si/c-Si interface, derived from the data in Fig. 1. Results are shown for 6×10^{13}, 3×10^{14}, and 9×10^{14} 250 keV Er/cm^2 implants. The line serves to guide the eye.

apart from a fluence scaling factor. The profile for the highest fluence (7×10^{14} Er/cm^2) shows a shape identical to the other two for depths >90 nm. For shallower depths however, 2–3 times more trapping is observed than would be expected from simple scaling of the profiles for the lower fluence samples. This enhanced trapping agrees with the trapping observed in the RBS spectra for a similar concentration (9×10^{14} Er/cm^2) in Fig. 1(b) for $d<100$ nm.

IV. DISCUSSION

The data in Figs. 1–4 clearly indicate that the segregation coefficient is very concentration dependent. For example, the data for the low-fluence sample in Fig. 2 show a (deconvoluted) Er peak concentration in the segregation

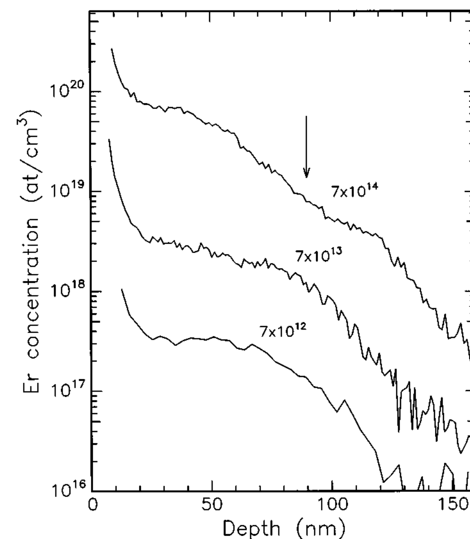

FIG. 4. Erbium concentration depth profiles derived from SIMS data. Results are shown for 7×10^{12}, 7×10^{13}, and 7×10^{14} 250 keV Er/cm^2, implanted in preamorphized Si(100), recrystallized at 600 °C for 15 min.

Downloaded¬15¬Sep¬2003¬to¬131.215.237.132.¬Redistribution¬subject¬to¬AIP¬license¬or¬copyright,¬see¬http://ojps.aip.org/japo/japcr.jsp

spike of 3×10^{20} Er/cm^3, and a concentration trapped in the crystal of only 3×10^{18} Er/cm^3 (see Fig. 4), hence $k=0.01$. However, data for the high-fluence sample in Fig. 2 indicate $k=0.20$. The threshold behavior in Fig. 3 indicates that this transition from low to high k takes place at a critical spike density of 6×10^{13} Er/cm^2. The analysis of Fig. 2 shows that this density corresponds to a segregation spike peak concentration of roughly 3×10^{20} cm^3.

The discontinuous incorporation behavior can be explained if the chemical potential of Er in a-Si is a discontinuous function of concentration. This could be understood if defects intrinsic to the a-Si network structure act as traps for the Er. Indeed, Cu and Pd diffusion studies[12,13] in a-Si with different defect densities have shown that these defects determine the solubility of these impurities in a-Si. Much work has been devoted to the study of defects in a-Si, and a variety of different techniques has indicated that (possibly vacancy-type) defects can exist in the covalent a-Si random network to a concentration of typically 0.1–1.0 at. %.[14,15] In the context of this defect-trapping model, Er would then be easily soluble in a-Si for Er concentrations below the defect density. That then implies that for low Er concentrations in the segregation spike, the Er would nearly completely segregate (low k), as is observed. When the Er density in the segregation spike exceeds the defect density in a-Si, excess Er has to find an alternative site. As the local order in a-Si and c-Si is very similar, the energy associated to this excess configuration may be as high in a-Si as it is in c-Si. At this stage Er can go either into the crystal or stay on the amorphous side, and as a result k increases relative to the value for low Er concentrations, as is observed. The width of the Er plateau in Fig. 2 is equal to the typical diffusion distance of Er in a-Si ahead of the interface, D/v, with D the diffusivity and v the interface velocity. This leads to $D\approx10^{-13}$ cm^2/s, more than 4 orders of magnitude higher than the Er diffusivity in bulk a-Si.[7] Indeed, in the defect trapping model, the Er diffusion may be enhanced when the traps become filled so that they do not retard the diffusion.[16]

From the Er density measured in the segregation spike for the high-fluence sample (Fig. 2) we can make an estimate of the trap density: 3×10^{20} Er/cm^3 (0.6 at. %), in agreement with independent estimates of the defect density.[12–16] This estimate is an upper limit because the Er density in the spike is the sum of trapped Er and excess Er diffusing ahead of the interface or towards the crystal. Defining the effective solubility (C_A) of Er in a-Si as equal to the trap density, an upper limit may be calculated for the solubility (C_C) of Er in c-Si: $C_C=kC_A$, with $k=0.01$. We find $C_C=3\times10^{18}$ Er/cm^3. This is an upper limit, as the value of k measured during crystallization is higher than the equilibrium value due to kinetic factors.

Finally, we note that our earlier work[6] on SPE of a-Si doped with slightly higher Er concentrations than those reported in this paper, has shown that the crystallization breaks down by the formation of crystal twins, once the Er concentration in the crystal exceeds 1.2×10^{20} Er/cm^3 (at 600 °C). Following the solubility arguments presented in this paper we now attribute this breakdown to the fact that at such high Er concentrations, well above the equilibrium solubility, it becomes energetically favorable to nucleate twins which can act as traps for the excess Er. It was found that the concentration at which breakdown occurs decreases with temperature (500 °C: 2×10^{20} cm^{-3}, 600 °C: 1.2×10^{20} cm^{-3}, 900 °C, 6×10^{19} cm^{-3}).[6,7] This may partly be explained by the fact that at high-temperature structural relaxation reduces the defect density in the a-Si network structure.[12–14] This then causes a reduction in the density of trap sites for Er, and therefore breakdown at lower Er concentrations.

V. CONCLUSION

In conclusion, we have studied the segregation and trapping of Er during solid-phase crystallization of amorphous Si on crystalline Si. The segregation coefficient depends strongly on the Er concentration at the interface. At Er interface areal densities below 6×10^{13} Er/cm^2 nearly full segregation to the surface is observed, with $k=0.01$. At higher Er densities, both segregation and trapping in the crystal are observed, with $k=0.20$. The results are consistent with a model in which it is assumed that defects in the a-Si near the interface act as traps for the Er.

ACKNOWLEDGMENTS

This work is part of the research program of FOM, and was made possible by financial support from NWO, IOP-Electro Optics, STW, and the SCOOP Program of the European Community. Bela Mulder and Salvo Coffa are gratefully acknowledged for stimulating discussion.

[1] G. L. Olson and J. A. Roth, Mater. Sci. Rep. **3**, 1 (1988).
[2] S. U. Campisano, E. Rimini, P. Baeri, and G. Foti, Appl. Phys. Lett. **37**, 170 (1980).
[3] J. Narayan, O. W. Holland, and B. R. Appleton, J. Vac. Sci. Technol. B **1**, 871 (1983).
[4] D. C. Jacobson, J. M. Poate, and G. L. Olson, Appl. Phys. Lett. **40**, 118 (1986).
[5] J. S. Custer, Michael O. Thompson, D. J. Eaglesham, D. C. Jacobson, and J. M. Poate, J. Mater. Res. **8**, 820 (1993).
[6] A. Polman, J. S. Custer, E. Snoeks, and G. N. van den Hoven, Appl. Phys. Lett. **62**, 507 (1993).
[7] J. S. Custer, A. Polman, and H. M. van Pinxteren, J. Appl. Phys. **75**, 2809 (1994).
[8] A. Polman, G. N. van den Hoven, J. S. Custer, J. H. Shin, R. Serna, and P. F. A. Alkemade, J. Appl. Phys. **77**, 1256 (1995).
[9] F. A. Trumbore, Bell Syst. Tech. J. **39**, 205 (1960).
[10] P. M. Zagwijn, A. M. Molenbroek, J. Vrijmoeth, G. J. Ruwiel, R. M. Uiterlinden, J. ter Horst, J. ter Beek, and J. W. M. Frenken, Nucl. Instrum. Methods Phys. Res. B **94**, 137 (1994).
[11] R. G. Wilson, F. A. Stevie, and C. W. Magee, *Secondary Ion Mass Spectrometry* (Wiley, New York, 1989).
[12] A. Polman, D. C. Jacobson, S. Coffa, J. M. Poate, S. Roorda, and W. C. Sinke, Appl. Phys. Lett. **57**, 1230 (1990).
[13] S. Coffa, J. M. Poate, D. C. Jacobson, and A. Polman, Appl. Phys. Lett. **58**, 2916 (1991).
[14] S. Roorda, W. C. Sinke, J. M. Poate, D. C. Jacobson, S. Dierker, B. S. Dennis, D. J. Eaglesham, F. Spaepen, and P. Fuoss, Phys. Rev. B **44**, 3702 (1991).
[15] G. N. van den Hoven, Z. N. Liang, L. N. Niesen, and J. S. Custer, Phys. Rev. Lett. **68**, 3714 (1992).
[16] S. Coffa, J. M. Poate, D. C. Jacobson, W. Frank, and W. Gustin, Phys. Rev. B **45**, 8355 (1992).

Downloaded¬15¬Sep¬2003¬to¬131.215.237.132.¬Redistribution¬subject¬to¬AIP¬license¬or¬copyright,¬see¬http://ojps.aip.org/japo/japcr.jsp